Vibrations and Buckling of Eccentrically Loaded Stiffened Cylindrical Shells

Vibrations and buckling of stringer-stiffened eccentrically loaded cylindrical shells are studied experimentally and results are compared with theoretical predictions

by A. Rosen and J. Singer

ABSTRACT—The influence of eccentricity of loading on the vibrations and buckling of stringer-stiffened shells is studied. An established nonlinear theory, which takes into account nonlinear prebuckling, is applied and the predictions are compared with experimental results. Two families of shells, one 'heavily' stiffened and the other 'moderately' stiffened, were tested but detailed results are presented only for the 'heavily' stiffened shells. In each family there are three identical shells, each with different eccentricity of loading. In all cases, different in-plane-boundary conditions are considered and correlated with experimental results.

List of Symbols

A_1 = cross-sectional area of stringers
b_1 = stringer spacing (distance between centers of stringers)
c_1 = width of stringer
d_1 = height of stringer
E = elastic modulus
e_1 = stringer eccentricity (distance from shell middle surface to stiffener centroid)
e_i = eccentricity of loading at one stringer at one end (distance from shell middle surface to the point of load application)
$\bar{e}$ = average eccentricity of loading (distance from shell middle surface to the point of load application)
f = frequency
h = thickness of shell
I_{11} = moment of inertia of stringer cross section about its centroidal axis
L = length of shell
M_x = moment resultant in axial direction
m = number of longitudinal half waves
N_x = axial membrane force resultant
n = number of circumferential waves
P = axial load
P_{cr} = buckling load
R = radius-to-shell middle surface
SS3 = simple-support boundary condition, $M_x = w = v = N_x = 0$
SS4 = simple-support boundary condition, $M_x = w = v = u = 0$
u, v, w = displacements in axial, circumferential and radial directions, respectively (radial direction positive inward)
Z = $(1 - \nu^2)^{1/2}(L/R)^2(R/h)$, Batdorf shell parameter
ν = Poisson's ratio
η_{t1} = torsional stiffness parameter of stringer
ϵ_m = axial bending strain
$\sigma_{.001}$ = 0.1 percent offset yield stress

Introduction

The effect of load eccentricity on the buckling of stiffened cylindrical shells has been studied in recent years by different investigators.[1-9] Load eccentricity is usually defined as the radial distance between the line of axial-load application and the shell midskin. These theoretical studies, and the experimental results of Refs. 1 and 9, showed that load eccentricity has considerable influence on the buckling load of stringer-stiffened shells. In Ref. 9, a parametric study was carried out in order to assess the influence of load eccentricity for different stiffener geometries, shell length and boundary conditions. The theoretical investigation was amplified by extensive tests on integrally stringer-stiffened cylindrical shells loaded eccentrically and having different boundary conditions.

The present study extends the work of Refs. 9, 11 and 14 and considers the influence of load eccentricity on the vibration of axially loaded stiffened shells both theoretically and experimentally. Two families are studied, one 'heavily stiffened' and the other 'moderately stiffened'. Only the results for the heavily stiff-

---

A. Rosen and J. Singer are Instructor and Professor, respectively, Department of Aeronautical Engineering, Technion–Israel Institute of Technology, Haifa, Israel.
The research reported has been sponsored in part by the Air Force Office of Scientific Research, through the European Office of Aerospace Research United States Air Force, under Grant 72-2394.

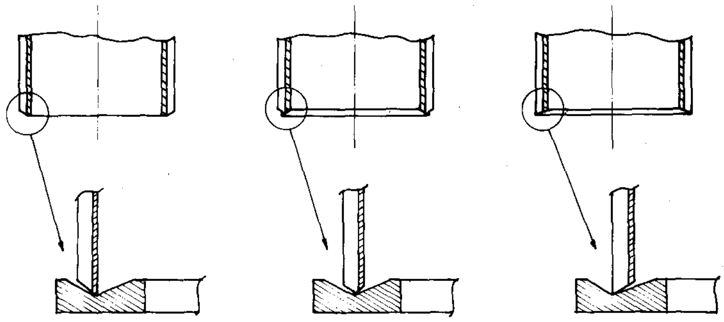

Fig. 1—Details of load application for different types of edges

ened shells are reported here in detail. The results for the moderately stiffened shells are presented in Ref. 18.

Theoretical Considerations

The studies of Ref. 9, compared the results of computations with different programs developed in Refs. 3, 4 and 8, indicated that the BOSOR 3 computer program[4] can be employed with confidence in the range of load eccentricities considered.

The BOSOR 3 computer program,[10] which takes into account nonlinear prebuckling deformations and eccentricity of loading, was, therefore, used in the calculations. As recommended in Ref. 5, for many cases the solution was repeated with different mesh sizes to ascertain that a properly converged solution had been found. For zero eccentricity, the results of BOSOR 3 were compared with those of a linear theory[11] which assumes a membrane prebuckling state of stress. In all computations, the stringers are assumed to be 'smeared' in a manner which takes their eccentricity into account, according to Ref. 12 or 13.

Experimental Setup and Procedure

The vibration excitation and measuring setup is the same as the one described in detail in Ref. 14. Here only a brief description is given. For excitation, an acoustic driver is installed inside the shell and is regulated by an outside oscillator. The measuring technique utilizes the noise emitted by the vibrating shells, which is picked up by a microphone positioned outside the shell. The resonance frequency is determined by Lissajous figures. With the resonance identified, the mode of vibration is mapped by scanning the shell with the microphone and taking noise readings as a function of the location. By keeping the circumferential or axial position constant and varying the other, one can plot the circumferential and axial mode shapes on X-Y recorders. The shell is loaded with a screw jack, and the load distribution is checked with an array of ten uniformly spaced strain gages. To check the moment and load transfer to the shell due to loading, four strips of five closely spaced strain gages were bonded in pairs near the edge of three of the shells. The strips in each pair were bonded on the two sides of the shell to permit separate measurement of bending strains or compressive strains.

Test Specimens

Six integrally stringer-stiffened shells were tested in the present test series. The specimens, which are similar to the shells of Refs. 14 and 15 were cut from 7075-T6, aluminum-alloy extruded tubes. The mechanical properties were verified to be $E = 73.6$ KN/mm^2 (10.6 $\times$ 10^6 lb/in.^{2}), $\sigma_{0.001} = 530$ N/mm^2 (76700 lb/in.^{2}) and $\nu = 0.3$. The shells with integral stringers were accurately machined by a process described in Ref. 15. The eccentricity of loading is achieved by applying the load through the stringers, as in Ref. 9. Specimens are, therefore, manufactured with three kinds of edges, as shown in Figs. 1 and 2. In the case of edge A, load is applied through the midskin of the shell; for edge B, load is applied through an intermediate point along the height of the stringers; and in the case of edge C, through the tip of the stringers. In all cases, special end rings (which may be seen in Fig. 1) are accurately fitted to the shell edges, which restrain the radial displacement of the shell edge or stringers.

The specimens were manufactured in triplet, consisting of three shells made from one blank, one with each of the three types of edges. Comparison was, therefore, between almost identical shells, as can be seen in Table 1.

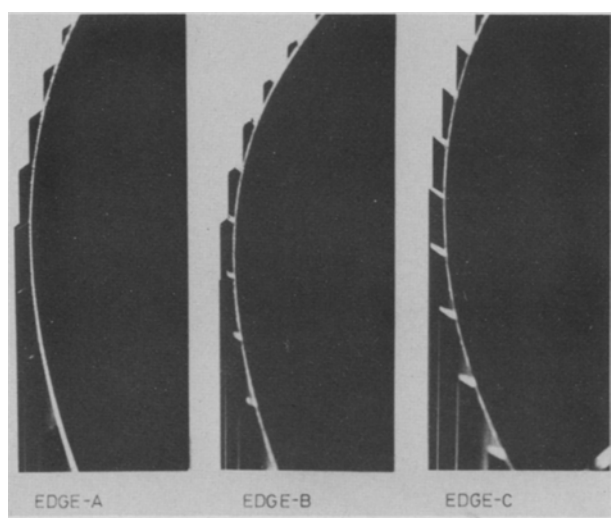

Fig. 2—Types of edges of shells

Results and Discussion

The dimensions of the shells are given in Table 1. There are two families of shells, one heavily stiffened—specimens RO-25, 26 and 27—and one moderately stiffened (medium stringers)—specimens RO-28, 29 and 30. Since the deviations in the dimensions of the shells are very small, a typical shell in each family was chosen for the calculations. For the heavily stiffened shells, this was RO-26, and for the moderately stiffened ones, RO-28.

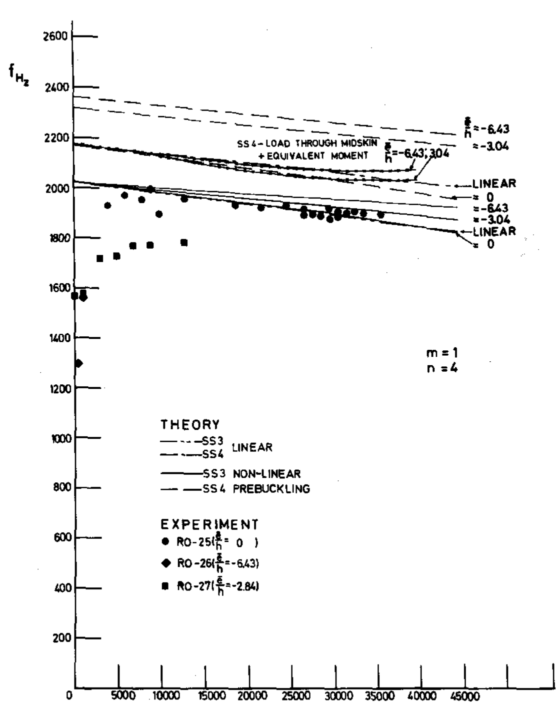

Fig. 3a—Frequency vs. axial load, "heavy" stringers ($A_1b_1h = 0.59$)

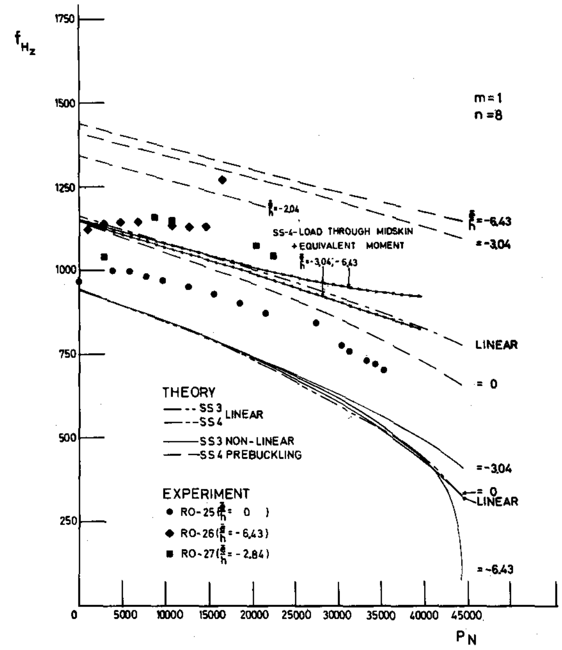

Fig. 3c—Frequency vs. axial load, "heavy" stringers ($A_1b_1h = 0.59$)

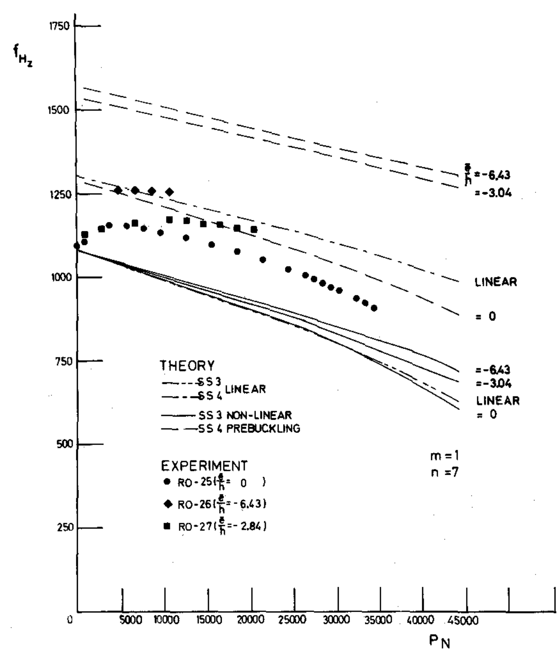

Fig. 3b—Frequency vs. axial load, "heavy" stringers ($A_1b_1h = 0.59$)

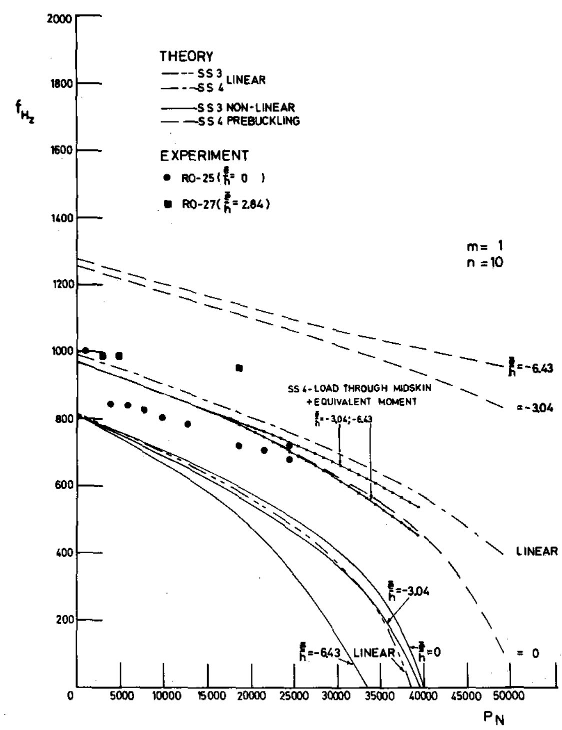

Fig. 3d—Frequency vs. axial load, "heavy" stringers ($A_1b_1h = 0.59$)

TABLE 1—GEOMETRICAL PROPERTIES OF SHELLS TESTED

Geometrical Property \ Shell	RO-25	RO-26	RO-27	RO-28	RO-29	RO-30
Radius to Shell middle surface R (mm)	120.13	120.13	120.13	120.13	120.13	120.13
Shell Thickness h (mm)	0.253	0.251	0.254	0.254	0.255	0.259
Shell Length L (mm)	130.0	130.0	130.0	130.0	130.0	130.0
Stiffener Width c_1 (mm)	0.90	0.90	0.90	0.90	0.90	0.90
Stiffener Height d_1 (mm)	1.505	1.488	1.480	0.979	0.974	0.980
Number of Stiffeners	84	84	84	84	84	84
Stiffener Eccentricity e_1 (mm)	−0.879	−0.870	−0.867	−0.617	−0.615	−0.620
R/h	474.8	478.6	473.0	473.0	471.1	463.8
L/R	1.082	1.082	1.082	1.082	1.082	1.082
Z	530.4	534.7	528.4	528.4	526.3	518.2
A_1/b_1h	0.596	0.594	0.584	0.386	0.383	0.379
e_1/h	−3.47	−3.47	−3.41	−2.43	−2.41	−2.39
I_{11}/b_1h^3	0.776	0.785	0.754	0.499	0.490	0.471
η_{t1}	6.598	6.678	6.375	3.099	3.025	2.943

7075 Aluminum Alloy, E = 73.6 KN/mm², ν = 0.3, Specific gravity = 2.80

Details of all the results are given in Ref. 18, whereas here, in the case of vibrations, only the heavily stiffened shells are discussed in detail. The discussion of buckling and the conclusions, on the other hand, summarize the results from all the specimens.

In the calculations, two kinds of boundary conditions were considered: SS3 ($M_x = w = v = N_x = 0$) and SS4 ($M_x = w = v = u = 0$). In all the cases, the results for SS4 boundary conditions were higher than those for SS3, as can be seen in Figs. 3 and 4.

For zero-load eccentricity, the predictions of linear theory (membrane prebuckling state of stress) may be compared with those of BOSOR 3 (that include nonlinear prebuckling). At zero load, there is practically no difference between the vibration frequencies predicted by the two theories for SS3 boundary conditions and for SS4 boundary conditions for small n [see Fig. 3(a)]. For $n > 6$ [Figs. 3(b)-3(d)] there is, however, a small difference for SS4, the predictions with nonlinear prebuckling being lower. After the application of load, small differences appear which grow with load and become significant for very high loads.

Calculations were performed for two values of nondimensional load eccentricity $(\bar{e}/h) = -3.04$ and -6.43, and some cases also for $(\bar{e}/h) = -2.04$ (for comparison with specimen RO-27). The difference in predicted frequencies due to eccentricity of loading grows with load and n. For SS3 boundary conditions and $n \leqq 7$ [Figs. 3(a), 3(b)] the lowest curve corresponds to zero eccentricity and the frequency increases with increasing load eccentricity. Then there is a change, [Fig. 3(c)], and for $n \geqq 10$, [Fig. 3(d)] the lowest frequency occurs at the largest eccentricity.

For the SS4 boundary conditions, the situation is different. In the calculations, the point of loading was also considered to be the supporting point of the shell (which corresponds to the experimental conditions). One notes in all Figs. 3 that the frequency for zero eccentricity is the lowest one, and that there is a significant increase in the frequency for $(\bar{e}/h) = -3.04$ and a smaller additional one as the eccentricity grows to $(\bar{e}/h) = -6.43$. Whereas, in the SS3 case at zero load, there is no difference due to eccentricity of loading, there are significant differences in the SS4 case at zero load, which are caused by the different supporting points. The differences grow with load, but this increase is smaller than the corresponding

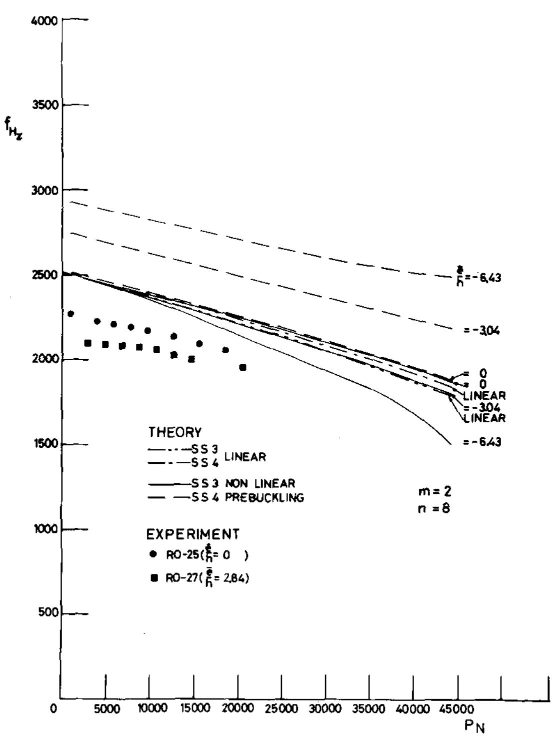

Fig. 4—Frequency vs. axial load, "heavy" stringers (A_1b_1h = 0.59)

one in the SS3 case. Because of the importance of the supporting point for SS4 boundary conditions, another set of calculations was performed. In these calculations, the load is applied through the midskin and the equivalent moment is added with the supporting point remaining at the midskin, with SS4 boundary conditions. The calculations were carried out for $n = 4, 8, 10$ [see Figs. 3(a), (c), (d)]. As expected, there is no difference at zero load due to eccentricity of loading, but it appears and grows with increase in load. For $n = 4, 8$ the frequency increases with eccentricity of loading, while for $n = 10$ the order changes and the lowest frequency corresponds to $(\bar{e}/h) = -6.43$. The differences in this case are much smaller than in the former case of SS4, in which supporting and loading points coincide.

The experimental results are also presented in Figs. 3(a)-3(d). Shell RO-25 was loaded through the midskin in the manner established in previous buckling tests at Technion, (see Refs. 15-17), edge A in Fig. 1. Shells RO-26 and 27 were with edges C and B, respectively, of Fig. 1 and were loaded eccentrically. With these edges, the line through which the load is introduced changes during load application due to yielding of the tips of the stringers, as in Ref. 9. This tends to move the line of action inward and to decrease the eccentricity. On the other hand, the tips of the stringers bend slightly outward during loading, which increases the eccentricity. These two effects are in opposite directions and their relative magnitudes cannot be predicted well. Therefore, before loading and after buckling, the specimen is placed on the table of a high-power magnifying comparator, and the distances from stringer tip before loading and from the center of the yielded area of the stringer after buckling to the midskin $\bar{e}_i$, are measured. The measurement was carried out separately for all the stringers at both edges and the average of the measurements was taken as the load eccentricity before and after loading. For shell RO-26, the nondimensional eccentricity before loading was $(\bar{e}/h) = -6.43$ and, after buckling, $(\bar{e}/h) = -5.66$. Note that the change in $(\bar{e}/h)$ due to loading is relatively small. For shell RO-27 the eccentricity before loading was $(\bar{e}/h) = -2.84$ and after buckling it was found to be $(\bar{e}/h) = -2.04$. For the vibration studies the experimental load eccentricities in Figs. 3 and 4 are therefore taken as -6.43 and -2.84.

It should be pointed out that, for these simple-support type of experimental boundary conditions, the shell has not yet 'settled' at zero and small loads and, hence, the boundary conditions are not well defined at small loads. One must, therefore, examine the experimental results at low loads very carefully.

From Fig. 3(a) one observes that for $n = 4$, the eccentricity of loading yields experimentally lower frequencies than predicted for SS3 boundary conditions. For $n = 7$ [Fig. 3(b)], the experimental behavior is similar to that predicted for SS4, RO-25, (with $(\bar{e}/h) = 0$) having the lowest frequencies and those of RO-27 (with $(\bar{e}/h) = -2.84$) and RO-26 (with $(\bar{e}/h) = -6.43$) above them, respectively. For higher circumferential wave numbers, the SS4 predictions are approached further with increasing n. Note that there are fewer experimental results for high circumferential wave numbers because they are more difficult to detect.

Typical results for two axial half waves appear in Fig. 4. At zero load eccentricity the difference between SS3 and SS4 boundary conditions is small, both for linear theory and nonlinear theory. This difference increases with n and load, the prediction of linear theory being always lower.

The nonlinear theory predicts here for $m = 2$ and SS3 boundary conditions lower frequencies for outward eccentricity of loading. For SS4 boundary conditions, the same eccentricity of loading results in higher frequencies, as in the case of $m = 1$. As before, this effect exists also at zero load, due to the different supporting points. The increase of this difference with load is very small compared to that for SS3 boundary conditions. The experimental results for two axial half waves are also shown in Fig. 4. (For RO-26, no results were obtained for $m = 2$, $n = 8$; the few results recorded with $m = 2$ were for $m = 2$, $n = 10$; see Fig. 6(d) of Ref. 18.) The experimental results in Fig. 4 are lower than the values predicted by theory and outward load eccentricity yields lower frequencies. Similar results were obtained for other values of n [see Figs. 6(a), 6(c)-6(e) and Figs. 11(a)-11(h) of Ref. 18] but, in general, the experimental results for $m = 2$ do not exhibit the clear trends shown by those for $m = 1$.

Figure 5 shows the influence of eccentricity of loading on the buckling loads. The theoretical curves were computed with BOSOR 3[10] for nonlinear prebuckling. For SS3 boundary conditions there is little effect up to an outward load eccentricity of $(\bar{e}/h) = -2.5$, where a shallow maximum occurs. For larger outward load eccentricities the buckling load decreases and also the mode of buckling changes. For SS4 boundary conditions there is initially a steep rise

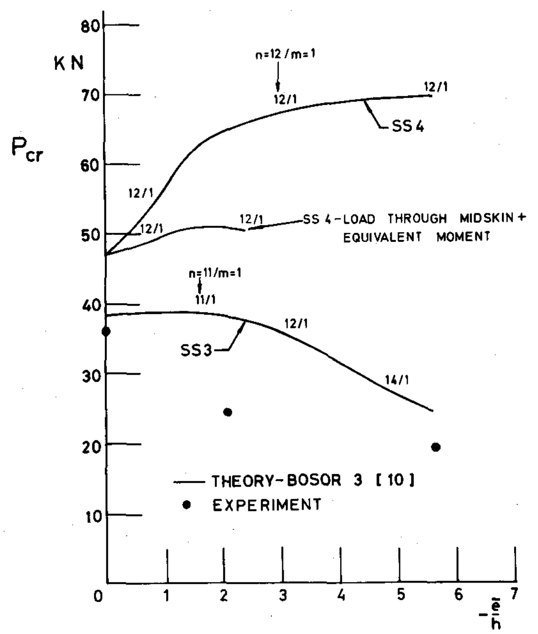

Fig. 5—Influence of eccentricity of loading on buckling loads, "heavy" stringers ($A_1 b_1 h = 0.59$). (Reproduced from Ref. 19)

in the buckling load with increase of outward eccentricity up to $(\bar{e}/h) = -1.5$. After that, the increase is more moderate. The case of SS4 boundary conditions with load through midskin plus an equivalent moment is also plotted. This case differs from the former case of SS4 (with coinciding support and loading point) and is closer in its behavior to the SS3 case. We see that the theoretical influence of load eccentricity on the buckling load is similar to its influence on vibrations, especially for SS4 boundary conditions, where also for vibrations there is a steep rise in frequencies for small outward load eccentricity and a more moderate one for higher eccentricities.

The three experimental points are plotted in Fig. 5. The three shells buckled with $m = 1$, but exhibited different behavior near buckling. RO-25 buckled at 36.3 KN with 8 circumferential waves and the load dropped after buckling to 15.7 KN. Shell RO-26 showed noticeable bending before buckling. Buckling occurred at 19.5 KN (it was not so well defined and the number waves could not be counted). After buckling the load dropped only to 19.2 KN. The shell then continued to carry higher loads and the waves developed with increasing loads [see Fig. 6(a) at 20.6 KN and Fig. 6(b) at 21.1 KN]. At 20.6 KN and 21.1 KN there were approximately 12 waves. Shell RO-27 buckled at 24.5 KN with approximately 10 waves, and after buckling the load dropped to 22.0 KN. Note that for buckling calculations, the load eccentricity measured after buckling is employed, $(\bar{e}/h) = -5.66$ for RO-26 and $(\bar{e}/h) = 2.04$ for RO-27).

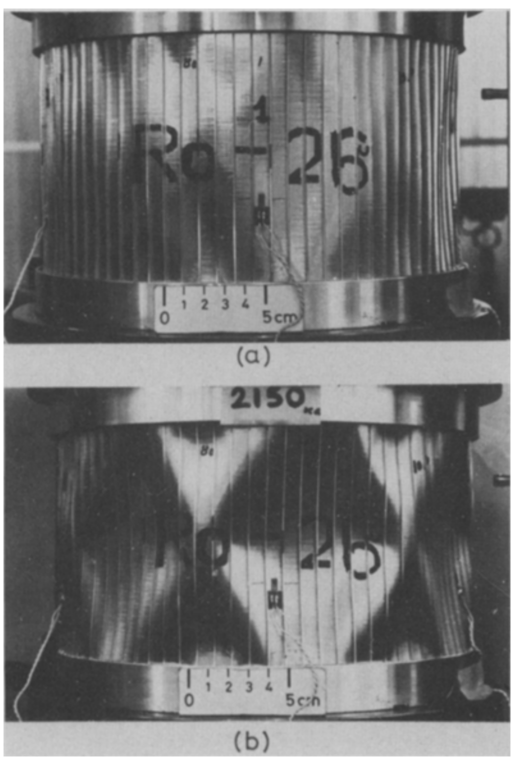

(a) AtP = 20.6 KN
(b) AtP = 21.1 KN

Fig. 6—Buckling patterns, shell RO-26 $\left(\frac{\bar{e}}{h} = -5.66\right)$

The experimental results reconfirm and emphasize the behavior observed in Ref. 9, that an increase in outward load eccentricity results in lower buckling loads but also in a much less violent buckling phenomenon.

The influence of eccentricity of loading on buckling for the moderately stiffened shells is discussed in detail in Ref. 18. The behavior is similar to that observed for the heavily stiffened shells in Fig. 5, except for some differences in the theoretical curves, which are exhibited also by the vibrations (see Figs. 12 and 10 of Ref. 18).

The group of moderately stiffened shells consists of RO-28 with zero load eccentricity, RO-30 with $(\bar{e}/h) = -1.87$ before loading and $(\bar{e}/h) = -2.10$ after buckling, and RO-29 with $(\bar{e}/h) = -4.35$ and -4.44 respectively.

For this group of shells, the transfer of load and moment to the shell was checked with pairs of five closely spaced strain gages. From plots of the axial vibration of axial compressive strain near an edge (see Fig. 13 of Ref. 18), the load diffusion is found to be very rapid for shells RO-29 and 30 and, at 13 mm from the edge, the values of compressive strain have almost reached their asymptotic value (measured at 44 m from edge). For shell RO-29, the one with largest outward load eccentricity, the diffusion is slower, as would be expected, but also in this shell the asymptotic value is reached fairly rapidly.

The axial variation of bending strain near an edge is shown in Fig. 7. As predicted, the bending moment at the edge is relatively small for shells RO-28 and 30 compared to that in shell RO-29. It is this larger edge moment in the shell with the appreciable outward load eccentricity, RO-29, that caused the reduction in buckling load and 'softening' of the buckling behavior.

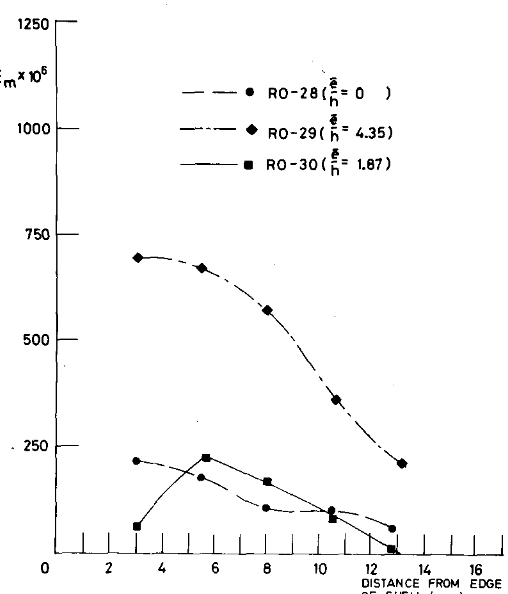

Fig. 7—Axial variation of bending strain near edge. (P = 15.7 KN)

Conclusions

Eccentricity of loading has a significant influence on the vibrations and buckling of stringer-stiffened shells, as predicted by theory and confirmed by experiments. Theory shows that this influence strongly depends on the boundary conditions and shell geometry. But for the geometries examined and external eccentricity of load, a few general conclusions can be made:

1. For SS3 boundary conditions, the influence of eccentricity of loading is negligible at small loads but increases with load. At low circumferential wave numbers, $n < 5$, the effect is small and outward eccentricity raises the frequency slightly. At high circumferential wave numbers $n \geqq 9$, large outward eccentricity of loading, $-\ (\bar{e}/h)\ > 2$ yields lower frequencies.
2. For SS4 boundary conditions the coincidence or noncoincidence of the point of load application with the supporting point was found to be important. When the two points coincide, the eccentricity of loading affects the vibrations even at zero load and the difference increase with load. As opposed to the case of SS3 conditions, for SS4 boundary conditions, outward eccentricity of loading always yields higher frequencies. The case of SS4 boundary conditions, with coinciding loading and supporting points, differs considerably from the case of SS4 boundary conditions with load applied through the midskin plus an equivalent moment in buckling calculations.
3. The experimental results for vibrations exhibit different behavior with variation in circumferential wave numbers. For small numbers of circumferential waves, the frequencies are even lower than the prediction for SS3 boundary conditions but, with higher circumferential wave numbers, the experimental results are higher than the SS3 predictions and approach those for the SS4 boundary conditions. The influence of the eccentricity of loading also changes qualitatively with circumferential wave numbers. Experiments show that for small numbers of circumferential waves, outward eccentricity of loading lowers the frequencies, while for higher numbers of waves this trend is reversed and larger outward eccentricity of loading results in higher frequencies.
4. The preceeding remarks relate to vibrations with one axial half wave. Eccentricity of loading has a less pronounced influence on the vibrations with two axial half waves. The experimental results for vibrations with two axial half waves are not as clearly defined as those for vibrations with one axial half wave.
5. The influence of eccentricity of loading on the buckling load also depends on the boundary conditions. This influence very much resembles that observed for vibrations. The experimental results indicate that, while an increase in outward load eccentricity lowers the buckling loads, it also results in a much less violent buckling phenomenon.
6. In the tests the possibility of a local out-of-plane freedom (in the radial direction) arises. Some calculations carried out to check the effect of weak local radial restraints showed, however, that the effect is small for vibrations and is even smaller for buckling.
7. The influence of nonlinear prebuckling deformations on the vibrations of stringer-stiffened shells is very small and may usually be ignored, except for loads close to buckling.

Acknowledgment

The authors wish to thank H. Abramovits, A. Greenwald and A. Klausner for their dedicated assistance in the experimental work and data processing. They also wish to thank S. Nachmani, S. Fledel, Mrs. L. Spector and Mr. Azulai for their assistance, Mrs. D. Zirkin for the typing of the manuscript and Mrs. D. Rosen for preparation of the figures.

References

1. *DeLuzio, A., Stuhlman, C. E. and Almroth, B., "Influence of Stiffener Eccentricity and End Moment on Stability of Cylinders in Compression," AIAA Journal, 4 (5), 872-877 (May 1966).*
2. *Seggeike, P. and Geier, B., "Das Beulverhalten versteifter Zylinderschalen," Zeitschrift fuer Flugwissenschaften No. 15, Helft 12, 477-490 (December 1967).*
3. *Block, D. L., "Influence of Discrete Ring Stiffeners and Prebuckling Deformations on the Buckling of Eccentrically Stiffened Orthotropic Cylinders," NASA TN D-4283 (January 1968).*
4. *Almroth, B. O., Bushnell, D. and Sobel, L. H., "Buckling of Shells of Revolution with various Wall Constructions," NASA CR-1049, 1, Numerical Resuts (May 1968).*
5. *Almroth, B. O. and Bushnell, D., "Computer Analysis for Various Shells of Revolution," AIAA Journal, 6 (10), 1848-1855 (October 1968).*
6. *Stein, M., "Some Recent Advances in the Investigation of Shell Buckling," AIAA Journal, 6 (12), 2339-2345 (December, 1968).*
7. *Hutchinson, J. W. and Frauenthal, J. C., "Elastic Post-Buckling Behaviour of Stiffened and Barreled Cylinders," J. Appl. Mech., 36, Series E, (4), 784-790 (December 1969).*
8. *Chang, L. K. and Card, M. F., "Thermal Buckling Analysis for Stiffened Orthotropic Cylindrical Shells," NASA TN-D-6332 (April 1971).*
9. *Weller, T., Singer, J. and Batterman, S. C., "Influence of Eccentricity of Loading on Buckling of Stringer-Stiffened Cylindrical Shells," Thin-Shell Structures, Theory, Experiment and Design, ed. by Fung Y. C. and Sechler, E. E., Prentice-Hall, Englewood-Cliffs, NJ, 305-324 (1974).*
10. *Bushnell, D., "Stress, Stability and Vibration of Complex Shells of Revolution: Analysis and User's Manual for BOSOR 3, Lockheed Missiles and Space Co., Report N-5J-69-1, Samso TR-69-375 (Sept. 1969).*
11. *Rosen, A. and Singer, J., "Vibrations of Axially Loaded Stiffened Cylindrical Shells: Part I—Theoretical Analysis," TAE Report No. 162, Technion Research and Development Foundation Ltd., Haifa, Israel (February 1974).*
12. *Singer, J., Baruch, M. and Harari, O., "On the Stability of Eccentrically Stiffened Cylindrical Shells under Axial Compression," Int. J. of Solids and Structures, 2, 445-470 (1967). Also TAE Report No. 44, Technion Research and Development Foundation, Haifa, Israel (December, 1965).*
13. *Baruch, M. and Singer, J., "Effect of Eccentricity of Stiffeners on the General Instability of Stiffened Cylindrical Shells under Hydrostatic Pressure," J. of Mech. Eng. Sci., 5 (1), 23-27 (March 1963).*
14. *Rosen, A. and Singer, J., "Vibrations of Axially Loaded Stiffened Cylindrical Shells: Part II—Experimental Analysis," TAE Report No. 163, Technion—Israel Institute of Technology, Haifa, Israel (August 1973).*
15. *Weller, T. and Singer, J., "Experimental Studies on the Buckling of 7075-T6 Aluminum Alloy Integrally Stringer-Stiffened Shells," TAE Report No. 135, Technion Research and Development Foundation, Haifa, Israel (November 1971).*
16. *Singer, J., "The Influence of Stiffener Geometry and Spacing on the Buckling of Axially Compressed Cylindrical and Conical Shells," Theory of Thin Shells, Proc. of 2nd IUTAM Symp. on Theory of Thin Shells, Copenhagen, (September 1967), 234-263, Springer-Verlag, Berlin (1969).*
17. *Weller, T., Singer, J. and Nachmani, S., "Recent Experimental Studies on Buckling of Integrally Stiffened Cylindrical Shells under Axial Compression," TAE Report 100, Technion Research and Development Foundation, Haifa, Israel (February, 1970).*
18. *Rosen, A. and Singer, J., "Vibrations and Buckling of Eccentrically Loaded Stiffened Cylindrical Shells," TAE Report No. 205, Technion Research and Development Foundation, Haifa, Israel (June 1974).*
19. *Singer, J. and Rosen, A., "The Influence of Boundary Conditions on the Buckling of Stiffened Cylindrical Shells," presented at IUTAM Symp. on Buckling of Structures, Harvard University, June 17-21, 1974, to be published in the Proceedings.*